Chinese Journal of Catalysis 34 (2013) 1148–1158

available at www.sciencedirect.com

ScienceDirect

journal homepage: www.elsevier.com/locate/chnjc

Article

Modification of nanocrystalline HZSM-5 zeolite with tetrapropylammonium hydroxide and its catalytic performance in methanol to gasoline reaction

HE Yingping [a], LIU Min [a,*], DAI Chengyi [a], XU Shutao [b], WEI Yingxu [b], LIU Zhongmin [b], GUO Xinwen [a,#]

[a] *State Key Laboratory of Fine Chemicals, Department of Catalysis Chemistry and Engineering, School of Chemical Engineering, Dalian University of Technology, Dalian 116024, Liaoning, China*

[b] *Dalian Institute of Chemical Physics, Chinese Academy of Sciences, Dalian 116023, Liaoning, China*

ARTICLE INFO

Article history:
Received 30 November 2012
Accepted 18 March 2013
Published 20 June 2013

Keywords:
Nanocrystalline HZSM-5
Zeolite
Tetrapropylammonium hydroxide
Methanol to gasoline

ABSTRACT

Nanocrystalline ZSM-5 zeolite was modified with tetrapropylammonium hydroxide (TPAOH) solution. The effect of the TPAOH treatment time on the catalytic performance of HZSM-5 was investigated in methanol to gasoline (MTG) reaction. The modified samples were characterized using X-ray diffraction, scanning electron microscopy, ^{27}Al and ^{29}Si magic-angle spinning nuclear magnetic resonance spectroscopy, X-ray photoelectron spectroscopy, N_2 adsorption, and NH_3 temperature-programmed desorption. The HZSM-5 structure was basically unchanged after modification, but the relative crystallinity increased and the crystal morphology was more regular. The Brunauer-Emmett-Teller surface area, the micropore surface area, the surface Si/Al ratio, and the amount of strong acid sites increased; this might be caused by desilication and dealumination, and secondary crystallization of the zeolite during the treatment. The stability of the catalyst was significantly improved after modification, as reflected by the increased lifetime from 70 h to above 170 h in MTG reaction. The catalyst lifetime increased with increasing TPAOH treatment time. Hydrogen transfer reactions became faster and led to more isoparaffins and less olefins in the liquid products.

1. Introduction

The methanol to gasoline (MTG) process [1–3] was first discovered and developed by researchers at Mobil in 1976, based on coal or natural gas as the raw material and conversion of synthesis gas to methanol. In the MTG process, crude methanol is transformed into high-octane and high-quality gasoline, which contains no sulfur, chlorine, or other impurities and has a good anti-knock performance. With the shortage of world oil resources and the overproduction of domestic methanol, methanol is becoming a new source of fossil-fuel raw materials.

ZSM-5 zeolite is usually used as the catalyst in the MTG process. The ZSM-5 zeolite framework contains two interconnected pore systems, i.e., straight channels (0.51 nm × 0.55 nm) and zigzag channels (0.53 nm × 0.56 nm), creating a three-dimensional network. The presence of micropores gives rise to the use of zeolites as shape-selective catalysts. In ZSM-5, diffusion of molecules that have a greater critical size than that of durene is difficult, leading to high selectivity in MTG. However, the stability of the parent HZSM-5 is not satisfactory be-

* Corresponding author. Tel/Fax: +86-411-84986134; E-mail: lium@dlut.edu.cn
# Corresponding author. Tel/Fax: +86-411-84986133; E-mail: guoxw@dlut.edu.cn

This work was supported by the New Century Excellent Talent in University, China (NCET-04-0268) and the Plan 111 Project of the Ministry of Education of China.
DOI: 10.1016/S1872-2067(12)60579-8 | http://www.sciencedirect.com/science/journal/18722067 | Chin. J. Catal., Vol. 34, No. 6, June 2013

cause of easy coke deposition on the strong acid sites on the surface [4]. It is therefore important to improve the catalyst stability.

Alkaline modification, i.e., desilication by treatment in an alkaline medium, is a very suitable and reproducible method for obtaining mesoporous ZSM-5 zeolites with improved diffusivity and catalytic cracking ability, and has attracted growing interest in zeolite applications in recent years. Currently, an inorganic NaOH solution is generally used as the alkaline medium. Bjørgen et al. [5] reported a significant improvement in the catalyst lifetime and a strongly enhanced selectivity towards the desired gasoline fraction, i.e., more aromatic and paraffinic compounds in the products, for HZSM-5 samples treated with NaOH solution. The results were rationalized by the development of acidity, improved crystallinity, and mesopore formation. Ogura et al. [6] and Suzuki et al. [7] found changes in the adsorption curves and pore size distributions for MFI zeolites modified with NaOH solution, leading to increased catalytic activity. Groen et al. [8,9] reported the formation of accessible intracrystalline mesopores in HZSM-5 as a result of selective removal of framework silicon by controlled desilication with NaOH. Ni et al. [10] prepared a hierarchical mesoporous Zn/ZSM-5 zeolite catalyst by NaOH treatment and Zn impregnation, giving significant improvements in the catalyst lifetime and liquid hydrocarbon yield in the MTG reaction. Xiao et al. [11] studied NaOH-treated mordenite containing a template and obtained increased isobutene conversion for ethyl *tert*-butyl ether synthesis. At present, organic alkaline treatment is usually used for TS-1. Compared with inorganic alkaline treatments, organic alkaline treatments give more moderate modifications and are more easily controlled. Mao et al. [12] found that the structure of TS-1 was basically unchanged after modification with tetrapropylammonium hydroxide (TPAOH) solution, but internal corrosion occurred. The modified sample showed a significant improvement in catalytic performance in the hydroxylation of phenol and ammoxidation of methyl ethyl ketone. Xia [13] studied TPAOH-treated TS-1 and observed an improved performance in the ammoxidation of methyl ethyl ketone. To date, few organic alkaline modifications of ZSM-5 zeolites have been reported.

In this work, we modified nanocrystalline ZSM-5 zeolite by TPAOH treatment and investigated its catalytic performance in MTG reaction and its physical and chemical properties.

2. Experimental

2.1. Catalyst preparation

Nanocrystalline NaZSM-5 zeolite powder (SiO_2/Al_2O_3 molar ratio = 26, crystal size 70–100 nm), synthesized using the patented method [14], was treated with 0.1 mol/L TPAOH solution for 24, 48, or 72 h at 170 °C in an autoclave, followed by washing with deionized water and filtering. After drying and calcination, the samples were ion exchanged three times with 0.4 mol/L NH_4NO_3 solution for 2 h at 75 °C, followed by washing, filtering, drying at 100 °C, and calcination in static air at 540 °C for 4 h. The obtained TPAOH-treated nanocrystalline HZSM-5 samples were designated HZ (no treatment), T24-HZ (treated for 24 h), T48-HZ (treated for 48 h), and T72-HZ (treated for 72 h). Strips of the TPAOH-treated nanocrystalline HZSM-5 samples were obtained by extruding mixtures of the TPAOH-treated nanocrystalline HZSM-5 samples with alumina (weight ratio of HZSM-5:Al_2O_3 = 4:1), followed by washing, drying at 100 °C, and calcination in static air at 540 °C for 4 h. The obtained samples were designated nHZ, T24, T48, and T72.

2.2. Catalyst characterization

X-ray diffraction (XRD) patterns were recorded using a Rigaku D/max-2400 diffractometer at a scanning rate of 6°/min from 5° to 50°. The crystal sizes and morphologies of the samples were examined using scanning electron microscopy (SEM; JEOL JSM-5600 LV). ^{27}Al and ^{29}Si magic-angle spinning nuclear magnetic resonance (MAS NMR) spectra were recorded using a Bruker Avance III 600 spectrometer. ^{27}Al MAS NMR spectra were recorded at a resonance frequency of 156.4 MHz with a spinning rate of 12 kHz, using a 0.75 μs ($\pi/8$) pulse with a 2 s recycle delay; chemical shifts were referenced to 3-(trimethylsilyl)-1-propanesulfonic acid sodium salt. ^{29}Si MAS NMR spectra were recorded at a resonance frequency of 119.2 MHz with a spinning rate of 8 kHz, using a 4 μs ($\pi/2$) pulse with a 2 s recycle delay; chemical shifts were referenced to $NH_4Al(SO_4)_2{\cdot}12H_2O$. X-ray photoelectron spectroscopy (XPS) was performed using a VG K-Alpha photoelectron spectrometer using Al K_α radiation. Surface area and pore size distribution were obtained with a Quantachrome AUTOSORB-1 analyzer using low-temperature N_2 adsorption. The adsorption capacities of *n*-hexane and cyclohexane were measured at 25 °C using a flow adsorption method. The acidic properties of the samples were obtained with a Quantachrome CHEMBET 3000 instrument using the NH_3 temperature-programmed desorption (TPD) method.

2.3. Catalytic tests

The prepared catalysts were tested for MTG in a continuous-flow fixed-bed reactor at atmospheric pressure. The HZSM-5 catalyst (1.0 g, 20–40 mesh) was placed in the center of the stainless-steel tubular reactor and γ-Al_2O_3 (1.0 g) was placed above it, separated by a layer of alumina balls. The weight hourly space velocity was 2.0 h^{-1}, and the reaction temperature was 380 °C. The effluent from the reactor was separated into gaseous and liquid products using ice-water.

Analysis of the gaseous products was performed using a Tianmei GC 7890F gas chromatograph equipped with an HP-PLOTQ capillary column (30 m × 4 mm), and the organic phase of the liquid product was analyzed using the GC 7890F gas chromatograph equipped with an OV-101 capillary column (50 m × 0.23 mm × 0.50 μm), with quantitative analysis using PONA software. The conversion of methanol to hydrocarbon products (dimethyl ether (DME) was considered to be reactant), X_M, is defined as X_M = (1 − the molar percentage of methanol in the effluent/the molar percentage of methanol in the reactant) × 100%.

3. Results and discussion

3.1. Catalyst characterization

Figure 1 shows the XRD patterns of the HZSM-5 samples. The number of peaks and the peak positions did not change after TPAOH treatment. The peak intensities at both low (2θ = 7.8° and 8.7°) and high (2θ = 22.9°, 23.6°, and 24.3°) diffraction angles increased slightly. This indicates that the TPAOH treatment did not adversely affect the crystal structure, and the relative crystallinities of the modified samples increased slightly, probably as a result of changes in an unstable phase. Li et al. [15] modified a ZSM-5 zeolite in a mixed alkaline aqueous solution of TPAOH and an inorganic base, NaOH, and found that the relative crystallinity of the zeolite increased with increasing TPA^+/OH^- ratio, indicating that the TPAOH modification is controllable.

Figure 2 shows SEM images of the HZSM-5 samples before extrusion. It can be seen that the crystal morphology was more regular and the crystals were larger after TPAOH treatment. These results are contrary to some published papers [6,7,9,10], which reported that the zeolite angles disappeared, the edges blurred, and the surfaces became rougher after NaOH treatment. These results are also different from those in another report [15], which showed that the zeolite surface became rougher with the increasing TPA^+/OH^- ratio after treatment with a mixed alkaline aqueous solution of TPAOH and NaOH. This shows that the inorganic base, NaOH, had a particularly strong influence on the zeolite, whereas the organic alkaline TPAOH had a more moderate influence and stabilized the zeolite structure. The TPAOH solution acts as a lye and can lead to the removal of framework silicon as well as framework aluminum. Also, acting as a template, the TPAOH solution may lead to secondary crystallization of amorphous species, non-framework silicon, and non-framework aluminum on the zeolite surface. Consequently, the relative crystallinity of the sample increased and the crystal size increased after TPAOH treatment. Huang [16] observed secondary crystallization when TS-1 was treated with TPAOH solution, and the crystal grains became more regular and some new crystal grains appeared after modification.

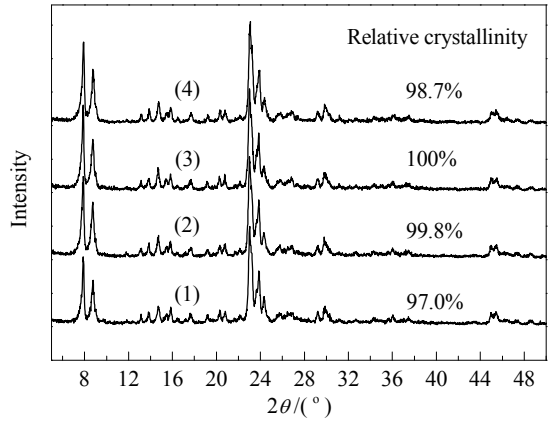

Fig. 1. XRD patterns of HZSM-5 with different TPAOH treatment time. (1) nHZ; (2) T24; (3) T48; (4) T72.

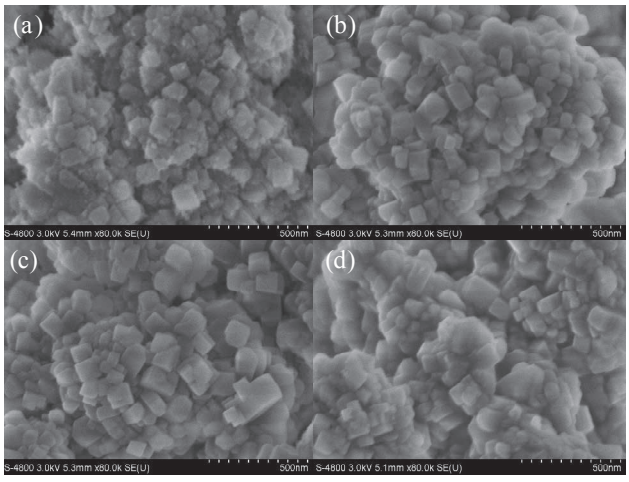

Fig. 2. SEM images of HZSM-5 with different TPAOH treatment time before extrusion. (a) HZ; (b) T24-HZ; (c) T48-HZ; (d) T72-HZ.

Figure 3(a) shows the ^{27}Al MAS NMR spectra of the HZSM-5 samples before extrusion. The spectra of all the samples are characterized by an intense and sharp signal at δ = 54, and a weaker and broad signal at δ = 0, arising from tetrahedrally coordinated framework aluminum and six-coordinated non-framework aluminum, respectively. For the HZ sample, there is a signal at δ = 37 attributed to five-coordinated framework aluminum. For the T24-HZ sample, the signal from five-coordinated framework aluminum decreases significantly, and the signal from non-framework aluminum increases significantly, clearly indicating removal of aluminum from the

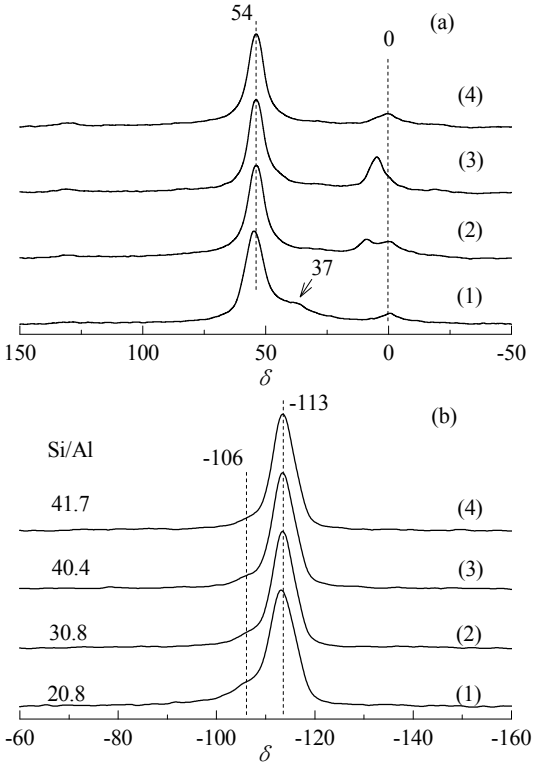

Fig. 3. ^{27}Al (a) and ^{29}Si (b) MAS NMR spectra of HZSM-5 with different TPAOH treatment time before extrusion. (1) HZ; (2) T24-HZ; (3) T48-HZ; (4) T72-HZ.

lattice. For the T48-HZ sample, the signal from non-framework aluminum increases further, showing that removal of aluminum from the lattice continues to occur. For the T72-HZ sample, the signal from non-framework aluminum decreases significantly, indicating the end of dealumination and the conversion of non-framework aluminum to framework aluminum.

Figure 3(b) shows the ^{29}Si MAS NMR spectra of the samples before extrusion. All the samples have signals at δ = −113 and −106, attributed to framework Si(OSi)$_4$ (Q4) and Si(OSi)$_3$(OAl) (Si1Al), respectively. For the T24-HZ sample, the framework Si/Al ratio increases from 20.8 to 30.8 compared with the HZ sample as a result of removal of framework aluminum, in agreement with the ^{27}Al MAS NMR spectra. For the T48-HZ sample, the framework Si/Al ratio further increases to 40.4, showing that removal of aluminum from the lattice is still occurring. For the T72-HZ sample, the framework Si/Al ratio changes little compared with the T48-HZ sample, increasing from 40.4 to 41.7. Based on a combination of these results and the ^{27}Al MAS NMR spectra, it can be concluded that secondary crystallization of the zeolite occurs when the TPAOH treatment time is longer than 48 h, resulting in migration of non-framework aluminum and non-framework silicon to the zeolite surface and their transformation into framework species. Analysis of the framework Si/Al ratio shows that the migration rate of non-framework silicon is faster than that of non-framework aluminum, especially in the treatment stage from 24 to 48 h.

Figure 4 shows the Si 2*p* and Al 2*p* XPS spectra of the HZSM-5 samples before extrusion. The surface Si/Al ratios of the samples obtained from the XPS spectra are shown in Table 1. For the HZ sample, the surface Si/Al ratio is 8.23; it is 13.2 for the T24-HZ sample, reaches a maximum, 17.9, for the T48-HZ sample, and decreases to 10.4 for the T72-HZ sample. The XPS spectra show that secondary crystallization of the zeolite does occur, making non-framework silicon migrate to the zeolite surface, resulting in an increase in the amount of framework silicon on the zeolite surface. Simultaneously, with increasing treatment time, some of the non-framework aluminum will migrate to the zeolite surface, and this is the reason for the decrease in the surface Si/Al ratio for the T72-HZ sample. Also, the results show that the migration of non-framework silicon is much easier, and the migration rate is faster, than those of non-framework aluminum during secondary crystallization, in agreement with the ^{27}Al and ^{29}Si MAS NMR results.

Table 1
Surface Si/Al ratios of HZSM-5 with different TPAOH treatment time before extrusion.

Sample	Surface Si/Al
HZ	8.2
T24-HZ	13.2
T48-HZ	17.9
T72-HZ	10.4

The pore properties of the HZSM-5 samples are shown in Table 2. The Brunauer-Emmett-Teller (BET) surface areas, micropore areas, micropore volumes, and total pore volumes of the samples all increase after TPAOH treatment, especially the micropore areas. The N_2 adsorption-desorption isotherms are shown in Fig. 5. The hysteresis loops in the isotherms of the modified samples are more pronounced and migrate upwards. These results are similar to those in some previous publications [5–9], which reported that these features were attributed to desilication and formation of new mesopores in ZSM-5 zeolite treated with NaOH solution. Compared with NaOH-treated samples, the changes in the hysteresis loops of the TPAOH-treated samples are less obvious, which may be the result of the moderate degree of modification caused by the TPAOH treatment, rather than new mesopore formation. However, TPAOH treatment can lead to an increase in the micropore volume, as shown by the data in Table 2. The increase in the BET surface area is mainly caused by dissolution of framework species [5,6]. The micropore area increase is possibly attributable to desilication, dealumination, and secondary crystallization of the zeolite during TPAOH treatment, resulting in amorphous species becoming framework species, and clearing of the channels.

Table 2
Pore properties of HZSM-5 with different TPAOH treatment time.

Sample	A_{BET} (m^2/g)	A_{ext} [a] (m^2/g)	A_{micro} [a] (m^2/g)	V_{micro} [a] (ml/g)	V_{total} [b] (ml/g)
nHZ	345	146	199	0.09	0.30
T24	373	141	232	0.10	0.31
T48	377	142	234	0.10	0.31
T72	373	147	226	0.10	0.31

[a] *t*-Method. [b] Volume adsorbed at p/p_0 = 0.99.

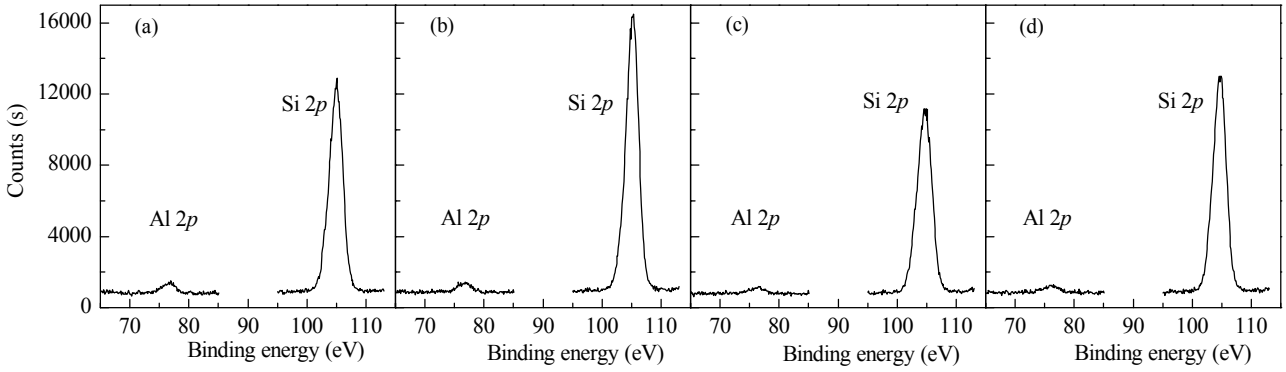

Fig. 4. Si 2*p* and Al 2*p* XPS spectra of HZSM-5 with different TPAOH treatment time before extrusion. (a) HZ; (b) T24-HZ; (c) T48-HZ; (d) T72-HZ.

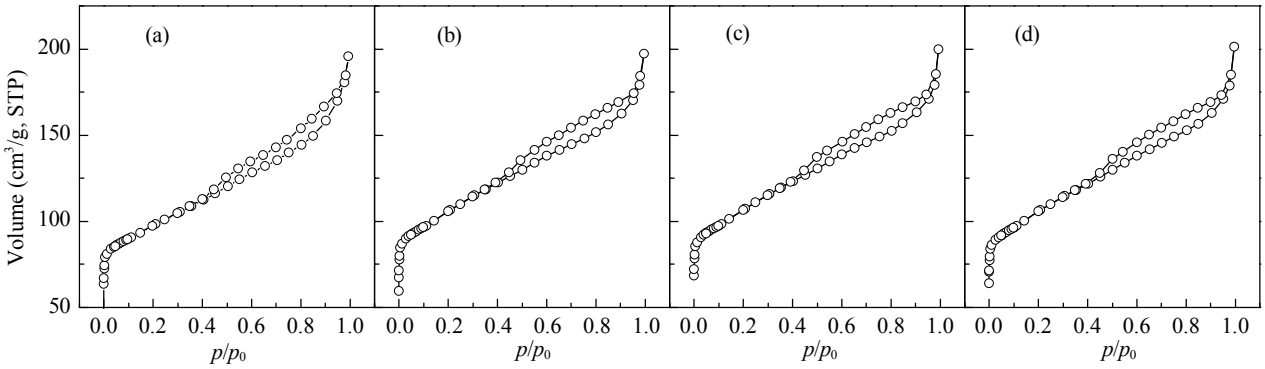

Fig. 5. N_2 adsorption-desorption isotherms of HZSM-5 with different TPAOH treatment time. (a) nHZ; (b) T24; (c) T48; (d) T72.

Figure 6 shows the adsorption curves of *n*-hexane and cyclohexane on the nHZ and T72 samples. The adsorption rates and capacities of both *n*-hexane and cyclohexane on the T72 sample are higher than those on nHZ. It can be concluded that the TPAOH treatment clears the channels of the HZSM-5 zeolite and increases the pore volume; this is consistent with the N_2 adsorption-desorption analysis.

Figure 7 shows the NH_3-TPD curves of the HZSM-5 samples. The high-temperature peak arises from strong acid sites and the occurrence of the low-temperature peak is related to the interaction of ammonia with different weak acid sites. It can be seen that the area of the low-temperature peak decreases, whereas that of the high-temperature peak increases, after TPAOH treatment, indicating a reduction in the number of weak acid sites and an increase in the number of strong acid sites. The number of weak acid sites increases with increasing TPAOH treatment time, whereas the number of strong acid sites first decreases and then increases. The two NH_3 desorption peaks shift towards lower temperatures after TPAOH treatment, showing a reduction in the strengths of the strong and weak acids. The TPAOH treatment time has less effect on the reduction in the acid strength. The change in acidity is caused by aluminum redistribution in the HZSM-5 zeolite, which may be attributed to desilication, dealumination, and secondary crystallization of the zeolite during TPAOH treatment. Presumably, the Al_2O_3 mixed with the nanocrystalline HZSM-5 during extrusion has an impact on the acidity of the HZSM-5 zeolite, leading to conversion from non-framework aluminum to framework aluminum during high-temperature calcination. However, further verification is needed.

3.2. Catalytic testing

Figure 8 shows the conversion of methanol to hydrocarbons as a function of time on stream for the four catalyst samples. The parent nHZ sample displays an activity above 98% within 70 h, and deactivation is rather fast, with the activity falling below 90% after 75 h on stream. The lifetime of the T24 sample is significantly better, as the conversion remains above 98% for 170 h, and deactivation is rather slow, with the activity falling below 90% after 200 h on stream. These effects are more pronounced for the T48 and T72 samples, i.e., the activity of the T48 sample falls below 90% after 210 h and the activity of the T72 sample falls below 90% after 230 h. It is concluded that the

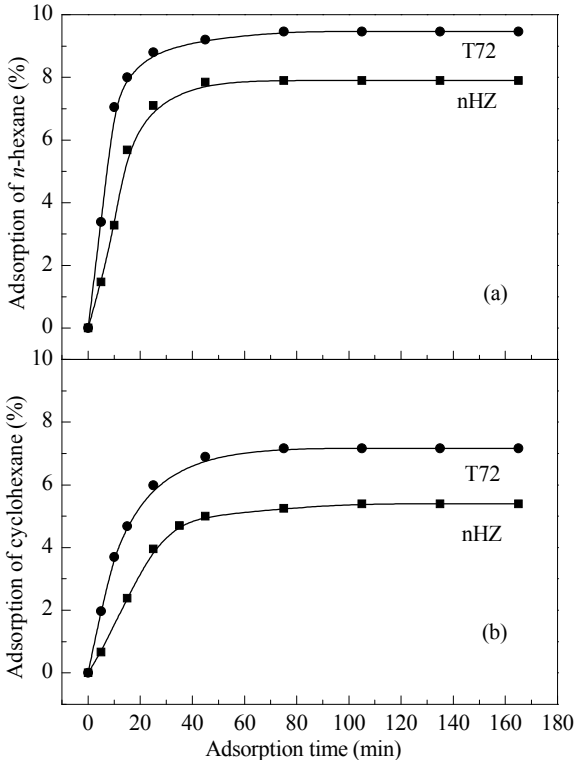

Fig. 6. Adsorption capacities of HZSM-5 before and after treatment with TPAOH for *n*-hexane(a) and cyclohexane(b).

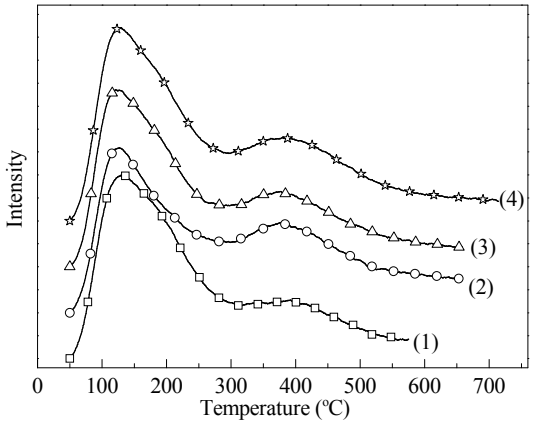

Fig. 7. NH_3-TPD profiles of HZSM-5 with different TPAOH treatment time. (1) nHZ; (2) T24; (3) T48; (4) T72.

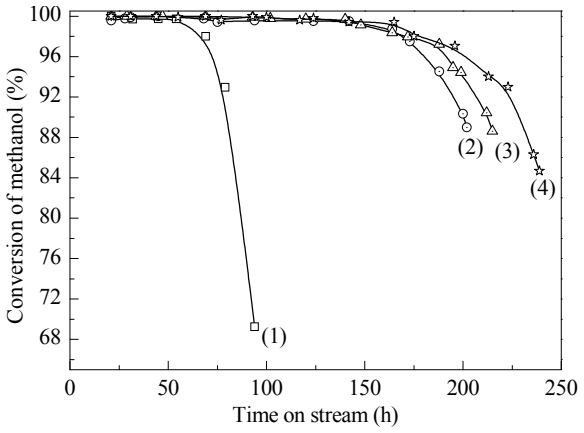

Fig. 8. Conversion of methanol/DME to hydrocarbons as a function of time on stream. (1) nHZ; (2) T24; (3) T48; (4) T72.

stability of the catalyst is significantly improved as a consequence of modification, and the lifetime of the catalyst increases with increasing TPAOH treatment time.

These results, in combination with the results of sample characterization, show that TPAOH treatment not only increases the BET surface area and exposes many more catalytic activity sites, improving adsorption and activation of reactant molecules, but also increases the micropore volume, clears the channels, and improves the diffusion capacity and coke tolerance; these are the reasons for the increased stabilities of the modified samples.

To obtain a more quantitative and precise measurement of the improvement in catalytic performance, the loosely defined concept of catalyst lifetime will be supplemented by the total conversion capacities. Based on Bjørgen's work [5], this is done by plotting the methanol conversion against the number of grams of methanol converted per gram of catalyst, and extrapolating to zero conversion, thus obtaining a value for the total capacity of the catalyst for MTG conversion until complete loss of activity; this is shown in Fig. 9. For the nHZ sample, the conversion capacity is 260 g(methanol)/g(catalyst). For the T24, T48, and T72 samples, the conversion capacities are 635, 680, and 750 g/g, respectively. The conversion capacity therefore

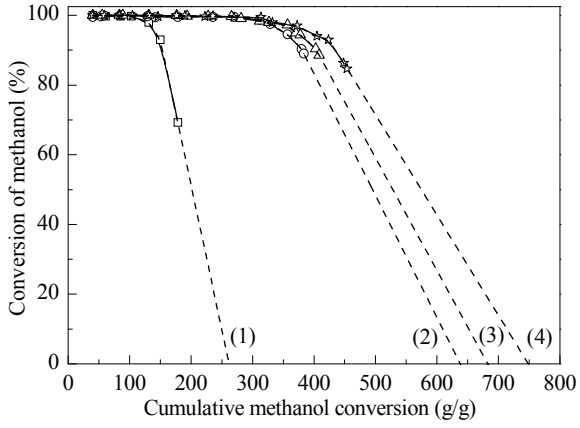

Fig. 9. Conversion of methanol plotted against the cumulative amount of methanol converted to hydrocarbons. Extrapolation to zero conversion gives the total conversion capacities of the four samples. (1) nHZ; (2) T24; (3) T48; (4) T72.

Table 3
Gaseous product distribution.

Sample	Product distribution (mol%)								C_3H_6/C_2H_4
	CH_4	C_2H_4	C_2H_6	C_3H_6	C_3H_8	C_4H_8	C_4H_{10}	C_5	
nHZ	7.6	11.5	6.1	8.6	9.7	26.0	6.0	13.9	0.8
T24	6.7	8.7	6.6	8.1	11.1	28.2	6.6	15.3	0.9
T48	6.7	9.1	6.8	8.4	10.2	27.7	6.8	15.5	0.9
T72	6.6	9.0	7.0	8.2	11.5	28.5	6.8	14.8	0.9

increases by a factor of about 3 as a result of the most severe treatment. In industry, catalytic reactions are seldom allowed to run until complete deactivation, but the calculated values show that the catalytic performance has been significantly improved by the TPAOH treatment.

Table 3 shows the gaseous product distribution, mainly light olefins and alkanes. Obviously, compared with the parent nHZ sample, the modified samples have less methane, more propane, and an increased propene/ethylene ratio in the gaseous products. Methane comes from the demethylation of aromatics and carbon precursors [17], so the more serious the carbon deposition, the more demethylation occurs, and the higher the methane formation. Some researchers have used the change in methane content as an indicator for measuring catalyst deactivation, i.e., a reduction in the methane content shows a slowing of the carbon deposition rate. We hypothesize that the diffusion of reactant and product molecules increases because the TPAOH treatment clears the channels of the HZSM-5 zeolite. Carbenium ions from propylene react with high olefins to give propane and dienes or aromatic compounds [18], as a result of hydrogen transfer reactions. The higher the propane content, the faster the hydrogen transfer reactions [19]. Hydrogen transfer is a biomolecular reaction, so it needs two acid sites with suitable and similar acid strengths. Some researchers [20] therefore consider that hydrogen transfer reactions may occur if the catalyst has a suitable space structure and active sites. After TPAOH treatment, the BET surface area and number of active sites increase, and the channels of HZSM-5 zeolite are cleared; these effects are beneficial to hydrogen transfer reactions between hydrocarbon molecules. The increase in the propene/ethane ratio is mainly caused by a decline in the ethane content, as reported by Bjørgen et al. [5], caused mainly by a decline in the rate of ethane formation via the aromatic-based hydrocarbon pool mechanism. As stated above, as the diffusivity increases and the time for which each aromatic molecule resides in the micropores is shortened, as a result of clearing the channels after TPAOH treatment, the probability of undergoing the reaction steps required for ethane formation diminishes.

Table 4 shows the liquid product distribution, mainly C_5–C_{10}

Table 4
Liquid product distribution.

Sample	Product distribution (vol%)				
	i-Paraffins	*n*-Paraffins	Olefins	Aromatics	Durene
nHZ[a]	31.3	4.1	9.7	51.7	4.0
T24[b]	33.5	3.9	8.4	50.2	5.3
T48[b]	34.4	3.2	7.8	50.8	4.3
T72[b]	33.1	3.5	7.6	51.5	4.3

[a] The mean value of 70 h. [b] The mean value of 170 h.

long-chain isoparaffins, olefins, and aromatics. Compared with the parent nHZ sample, the modified samples give more isoparaffins, less olefins, and a similar amount of aromatics. The main MTG reactions are as follows [21]: (1) generation of C_2–C_3 light olefins [22]; (2) generation of C_4–C_6 mixed olefins (the majority are isoolefins) via alkylation of C_2–C_3 light olefins and oligomerization reactions between C_2–C_3 light olefins and other olefins; (3) generation of aromatics via dehydrocyclization of C_6–C_{10} oligomers formed by oligomerization of linear C_2–C_5 olefins; (4) further isomerization and alkylation reactions of aromatics; and (5) hydrogen transfer reactions of isoolefins, which are not prone to oligomerization, to isoparaffins.

The main reason for the increase in the amount of isoparaffins and the decrease in the amount of olefins may be acceleration of the hydrogen transfer reactions. As mentioned above, TPAOH treatment improves the space structure and acidity of the samples, which strengthens the hydrogen transfer reaction activity. It can be seen from step (3) that aromatics are manufactured through polymerization and cyclization of light olefins, and this is associated with the pore structure and the number of strong acid sites in the zeolite. It has been reported that the generation of aromatics in MTG needs strong acidity [23,24]. As indicated by the NH_3-TPD results, TPAOH treatment increases the number of strong acid sites but reduces the strong acid strength. So, there is little change in the amount of aromatics. Moreover, more durene is seen for the modified samples, which is commonly attributed to the cleared channels assisting generation and diffusion of large molecules.

4. Conclusions

The physical and chemical properties of a nanocrystalline ZSM-5 zeolite modified with TPAOH solution were studied; the catalytic performance of the modified zeolite in MTG reaction was also investigated. The modification led to desilication, dealumination, and secondary crystallization of the zeolite, resulting in the migration of non-framework silicon and non-framework aluminum to the zeolite surface. The structures of the modified samples were basically unchanged, but the relative crystallinities increased and the crystal morphologies were more regular. The redistribution of framework silicon and framework aluminum caused an increase in the surface Si/Al ratio and the BET surface area, and the exposure of increased numbers of catalytic activity sites. The diffusion capacity and coke tolerance improved, which was attributed to an increase in the micropore volume and clearing of the channels. The stability of the catalyst was significantly improved, and the total conversion capacity increased by a factor of 3 as a consequence of the most severe treatment. Hydrogen transfer reactions became faster and led to more isoparaffins and less olefins in the liquid products.

References

[1] Stöcker M. *Microporous Mesoporous Mater*, 1999, 29: 3
[2] Zaidi H A, Pant K K. *Catal Today*, 2004, 96: 155
[3] Keil F J. *Microporous Mesoporous Mater*, 1999, 29: 49
[4] Campbell S M, Bibby D M, Coddington J M, Howe R F, Meinhold R H. *J Catal*, 1996, 161: 338
[5] Bjørgen M, Joensen F, Holm M S, Olsbye U, Lillerud K-P, Svelle S. *Appl Catal A*, 2008, 345: 43
[6] Ogura M, Shinomiya S-y, Tateno J, Nara Y, Nomura M, Kikuchi E, Matsukata M. *Appl Catal A*, 2001, 219: 33
[7] Suzuki T, Okuhara T. *Microporous Mesoporous Mater*, 2001, 43: 83
[8] Groen J C, Bach T, Ziese U, Paulaime-van Donk A M, de Jong K P, Moulijn J A, Perez-Ramirez J. *J Am Chem Soc*, 2005, 127: 10792
[9] Groen J C, Moulijn J A, Perez-Ramirez J. *J Mater Chem*, 2006, 16: 2121
[10] Ni Y M, Sun A M, Wu X L, Hai G L, Hu J L, Li T, Li G X. *J Nat Gas Chem*, 2011, 20: 237
[11] Xiao Q, Li Z Y, Sun X, Xiang S H. *Chin J Catal*, 2005, 26: 243
[12] Mao J B, Liu M, Li P, Liu Y, Guo X W. *J Fuel Chem Technol*, 2008, 36: 484
[13] Xia L Z. [MS Dissertation]. Dalian: Dalian Univ Technol, 2005

Graphical Abstract

Chin. J. Catal., 2013, 34: 1148–1158 doi: 10.1016/S1872-2067(12)60579-8

Modification of nanocrystalline HZSM-5 zeolite with tetrapropylammonium hydroxide and its catalytic performance in methanol to gasoline reaction

HE Yingping, LIU Min*, DAI Chengyi, XU Shutao, WEI Yingxu, LIU Zhongmin, GUO Xinwen*
Dalian University of Technology; Dalian Institute of Chemical Physics, Chinese Academy of Sciences

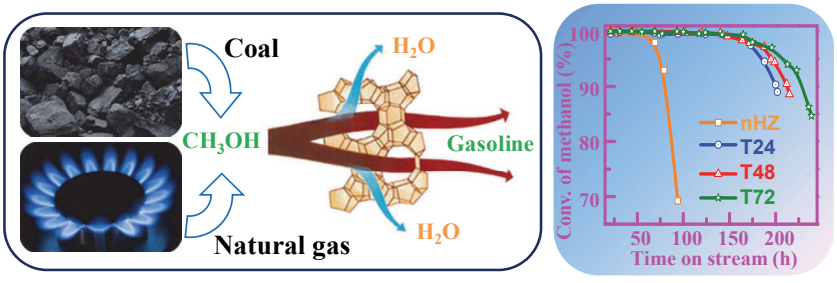

Tetrapropylammonium hydroxide treatment of the HZSM-5 zeolite improved the diffusion capacity and coke tolerance through desilication, dealumination, and secondary crystallization, reflected by the significantly increased catalyst lifetime.

[14] Wang X Q, Wang X S, Guo X W. CN Patent 1240193. 2000
[15] Li S, Li Y P, Di C Y, Zhang P F, Pan R L, Dou T. *J Fuel Chem Technol*, 2012, 40: 583
[16] Huang X L. [MS Dissertation]. Xiangtan: Xiangtan Univ, 2008
[17] Choudhary V R, Banerjee S, Panjala D. *Microporous Mesoporous Mater*, 2002, 51: 203
[18] Hao X, Du M X, Hu H M, Huang Z, Hu J N. *J Fuel Chem Technol*, 1995, 23: 28
[19] Zhu X X, Song Y Q, Li H B, Liu S L, Sun X D, Xu L Y. *Chin J Catal*, 2005, 26: 111
[20] Shen Z H, Fu Y M, Jiang M, Li S Y. *Chin J Catal*, 2004, 25: 227
[21] Gu B E, Wu Z X. Introduction to Industrial Catalysis. Beijing: Higher Edu Press, 1990. 138
[22] Blaszkowski S R, Van Santen R A. *J Am Chem Soc*, 1997, 119: 5020
[23] Zhu J H. *Chin J Catal*, 1993, 14: 294
[24] Wang J Y, Li W H, Hu J X. *J Fuel Chem Technol*, 2009, 37: 607